

# Certified Workspace Analysis of 3RRR Planar Parallel Flexure Mechanism

Denny Oetomo, David Daney, Bijan Shirinzadeh, Jean-Pierre Merlet

**Abstract**—This paper addresses the problem of certifying the performance of a precision flexure-base mechanism design with respect to the given constraints. Due to the stringent requirements associated with the applications of flexure-based precision mechanisms, it is necessary to be able to evaluate and certify the performance at the design stage, taking into account the possible sources of errors: such as fabrication tolerance and modeling inaccuracies in flexure joints. An interval-based method is proposed to certify whether various constraints are satisfied for all points within a required workspace. This paper presents the interval-based methodology and its implementation on a planar 3RRR parallel flexure-based manipulator.

## I. INTRODUCTION

**F**LEXURE jointed mechanisms [1] are widely utilised in precision positioning and manipulation devices [2], such as for pattern alignment in semiconductor fabrication, micro-assembly, micro-surgery, and various scanning microscopy techniques [3] [4].

Due to the high precision nature of the applications, there is a stringent demand on the performance of the manipulator. Currently, finite element methods are often employed to simulate the performance of the mechanism design, however this is limited in the types of criteria and does not allow a guaranteed solution or handling of uncertainties. It also tends to be computationally intensive. Topological information of the mechanism is often not considered and evaluation of the performance is on point-sampling basis. It is therefore difficult to guarantee that the robot satisfies the required constraints for all poses of its required workspace. There is also the issue of modeling inaccuracies in flexure mechanisms. For example, a revolute flexure joint is modeled as an ideal revolute joint. The deformation of the joint during deflection, however, produces residual translational motion. An attempt to take into account this residual motion was given in [5], where a revolute flexure joint was represented as a pair of revolute-prismatic joints. However, an accurate model for such parasitic motion is complex to obtain.

In this paper, an interval-based method is proposed to evaluate the various constraints and to certify whether or not they are achieved within the desired workspace of the flexure-based manipulator. As examples, we present the

cases of certifying two of the most common requirements in the design of a flexure precision mechanisms: (i) the range of reachable workspace and (ii) the achievable end-effector motion resolutions given the joint space resolutions. Furthermore, various uncertainties, including the inaccuracies of joint modeling and fabrication tolerances, can be accommodated as a bounded variations in the kinematic parameters. When a given workspace is certified as having satisfied all constraints, the certification is valid for all the continuous values within the bounds (as opposed to point-based sampling), even in the face of the above-mentioned uncertainties.

The work on obtaining the workspace of a manipulator has been presented in the past through geometrical approach [6] [7] and screw theory [8]. These methods define the boundaries of the manipulators geometrically and provide algebraic expressions to the boundary curves. The method presented in this paper obtains the same results as the analysis presented in [6] through interval methods. It is a constraint satisfaction certification technique, and as such, it is less specific to the manipulator. Through its generality, it is able to provide not only the boundary of reachable workspace, but is also useful in obtaining the workspace of the manipulator that satisfies other criteria, such as singularity free workspace and achievable motion resolution. It is, however, more computationally expensive.

The first part of the paper presents the interval-based method of certifying the solutions to each constraints in the flexure jointed mechanism. The second part presents the implementation results of the algorithm on a planar 3RRR parallel flexure-jointed mechanism.

## II. FLEXURE MECHANISMS

Flexure mechanism [1] is formed by significantly reducing the cross sectional area of a member at a particular point so that deflection through elastic deformation can be induced about that point while treating the rest of the member as ideal rigid bodies. As such, flexure joints do not suffer from any nonlinearities commonly associated with conventional joints such as friction, stiction, and backlash. They do, however, provide a much smaller range of displacement compared to conventional joints. Hence, they are suitable for precision manipulation.

The range of deflection that a flexure joint can undergo depends on the shear modulus of material and the design of the joint [9]. This range of deflection provides a natural bound to the joint displacement variables which then acts as

This study is conducted under Project ARES, a NEST-Adventure European Union project (EU contract no. 015653)

D. Oetomo, David Daney, and J-P. Merlet are with COPRIN project, INRIA Sophia-Antipolis. {david.daney, jean-pierre.merlet}@sophia.inria.fr

D. Oetomo is with the Dept. Mech. Engn., the University of Melbourne. doetomo@unimelb.edu.au

B. Shirinzadeh is with the Dept. Mech. Engn., Monash University. bijan.shirinzadeh@eng.monash.edu.au

a constraint in determining the achievable workspace of the end-effector in interval analysis method.

In this paper, we focus on the notch type joints [1], which (in ideal case) produce a one DOF revolute joint motion, without loss of generality in the algorithm presented for performance evaluation and the guarantee of constraint satisfaction. It is often modelled as a revolute joint, however it has been shown to display parasitic translational motion [5]. Other types of potential errors in the fabrication and assembly of a flexure jointed mechanism are outlined in [10].

### III. INTERVAL-BASED KINEMATICS METHOD

The goal of the algorithm is to evaluate the constraints placed on a given mechanism and to certify that they are satisfied for the associated end-effector workspace. In the notation,  $\mathbf{x}$  is a vector containing the task space variables and  $\mathbf{h}$  is a vector containing the design parameters of the mechanism (such as link lengths). The problem can therefore be formulated such that:

$$\{\forall \mathbf{x} \in [\underline{\mathbf{x}}, \overline{\mathbf{x}}], \forall \mathbf{h} \in [\underline{\mathbf{h}}, \overline{\mathbf{h}}]; C(\mathbf{x}, \mathbf{h}) \leq 0\} \quad (1)$$

where  $C(\mathbf{x}, \mathbf{h}) \leq 0$  are the constraints to be satisfied,  $\underline{\mathbf{x}}, \overline{\mathbf{x}}$  and  $\underline{\mathbf{h}}, \overline{\mathbf{h}}$  are the lower and upper bounds of the range of values in  $\mathbf{x}$  and  $\mathbf{h}$ , respectively. Generally, constraints in kinematic workspace problems can be formulated as inequalities  $C(\mathbf{x}, \mathbf{h}) \leq 0$ , such as in (1), which are easier to solve than equality constraints.

As an overview, the interval analysis method involves several main components:

- interval extension or evaluation of functions,
- testing against the constraints and obtaining the inner, outer, or boundary boxes,
- filtering, to obtain a sharper solution,
- branch-and-bound loop.

The goal of the strategy is to certify whether a particular range of workspace  $[\underline{\mathbf{x}}, \overline{\mathbf{x}}]$  and design parameters  $[\underline{\mathbf{h}}, \overline{\mathbf{h}}]$  constitute an inner or outer set of boxes to constraints  $C(\mathbf{x}, \mathbf{h})$ . If the range of the solution is too wide, often it is not possible to obtain a decision, in which case, filtering and branch-and-bound procedures are utilised. Filtering process sharpens the result of constraint evaluation while the branch-and-bound process splits the variables into smaller ranges and evaluates the constraints as a function of each subset of variable individually. The details of each component is given in the following sub-sections.

#### A. Interval Extension

The interval extension of variable  $x$  is defined as  $X$ , bounded within its lower and upper bound  $[\underline{x}, \overline{x}]$ , where  $\underline{x} \leq x \leq \overline{x}$ . The interval extension of a function is the evaluation of the function with interval variables. There are two major classes of interval extension: *natural extension*, where evaluation is done by substituting real variables with interval variables [11], and *Taylor-form extension* [12], which utilises the partial derivative of the function  $f(x)$ . Interval methods can be used conveniently to bound the remainder of truncated Taylor series. A common variation of the first order

Taylor-form is the *centered-form extension*, which evaluates  $f(x)$  around the centre point of  $X$ . In interval evaluation of a function, as numerical values are substituted into a function, relationship between variables are lost. Overestimation happens when multiple occurrences of the same variables within the function are regarded as independent variables. The evaluation of a function where all variables involved only appear once is *sharp* (within rounding errors), meaning it is bounded within the smallest possible “box”. A good introduction to the interval arithmetics can be found in [12].

#### B. Testing Against Constraints and Types of Solutions

After the evaluation, it is necessary to test whether a required constraint is satisfied in the system. In our problem, it is desired to verify whether the required performance constraint  $C(\mathbf{X}, \mathbf{H})$  of the mechanism is true for the set of given *workspace pose (variables)* of interest  $\mathbf{x} \in \mathbf{X}$  and *mechanism parameters (link lengths)*  $\mathbf{h} \in \mathbf{H}$ , as presented in (1). In the case of an inequality constraint, for example, a set of boxes  $(\mathbf{x}, \mathbf{h})$  is said to be:

- an *inner box* or *inner solution* of the constraint when  $\{\forall \mathbf{x} \in \mathbf{X}, \forall \mathbf{h} \in \mathbf{H}; \underline{C}_R \leq C(\mathbf{X}, \mathbf{H}) \leq \overline{C}_R\}$ , where  $\underline{C}_R$  and  $\overline{C}_R$  are the lower and upper bounds of the requirements for the constraints.
- an *outer box* is obtained when  $\{\forall \mathbf{x} \in \mathbf{X}, \forall \mathbf{h} \in \mathbf{H}; (C(\mathbf{X}, \mathbf{H}) \leq \underline{C}_R) \text{ or } (\overline{C}_R \leq C(\mathbf{X}, \mathbf{H}))\}$ ,
- $(\mathbf{x}, \mathbf{h})$  is a *boundary box* if it cannot be decided whether it is an inner or outer box.

#### C. Filtering

Filtering process enforces the consistency in the variables involved in a set of constraints. It is done by removing the segments in the interval variables involved that do not hold within the constraints. The filtering process is used to reduce the effect of overestimation on the interval extensions of functions.

Overestimation of an interval function makes it difficult to decide whether or not a set of interval variables satisfies the given constraints. Consistency filtering is therefore required to sharpen the resulting boxes. The process utilises the additional information contained within the mathematical equations or the physical constraints. In this paper, for example, a parallel mechanism is constructed out of several articulation chains that connect the base platform to the common moving platform, whose forward kinematics provides additional constraints that can be used to reduce the effect of overestimation. This is done, for example, by iteratively enforcing that the RHS and LHS (right and left hand side) of an equality evaluated to the same interval. This is termed the *2B consistency filtering* [13] [14]. Other filtering techniques are available such as 3B and interval Newton [15] [12] [16].

#### D. Branch-and-Bound

It is often difficult to conclude whether a given box  $(\mathbf{X}, \mathbf{H})$  constitute an inner or outer box when it is evaluated as a function of interval variables with large width. While filtering process contracts the box and attempts to obtain

TABLE I

SUMMARY OF ALGORITHM FOR WORKSPACE CONSTRAINT ANALYSIS  
WITH INTERVAL ANALYSIS.

1	<b>Initialise</b> empty lists $\mathcal{L}_{IN}$ , $\mathcal{L}_{OUT}$ , and $\mathcal{L}_B$ .
2	<b>Initialise</b> list $\mathcal{L}$ containing initial task space intervals (boxes) to be analysed.
3	<b>While</b> ( $\mathcal{L}$ not empty) <ul style="list-style-type: none"> <li>(a) Extract manipulator pose <math>\mathbf{X}_i</math> from list <math>\mathcal{L}</math>.</li> <li>(b) <b>Evaluate</b> constraints <math>C(\mathbf{X}, \mathbf{H})</math></li> <li>(c) <b>Test</b> <math>C(\mathbf{X}, \mathbf{H})</math> against the required performance <math>[\underline{C}_R, \overline{C}_R]</math>.</li> <li>(d) <b>Filtering</b> process is carried out if necessary.</li> <li>(e) Return whether <math>\mathbf{X}</math> constitutes an inner, outer, or boundary box.</li> <li>(f) <b>Case</b> result is inner, outer, or boundary box:                 <ul style="list-style-type: none"> <li>(i) <b>Case 1:</b> The solution lies within the ALL constraints <math>C(\mathbf{X}, \mathbf{H})</math> Remove <math>\mathbf{X}_i</math> from <math>\mathcal{L}</math> and add to list <math>\mathcal{L}_{IN}</math></li> <li>(ii) <b>Case 2:</b> The solution lies outside ANY of the constraints in <math>C(\mathbf{X}, \mathbf{H})</math> Remove <math>\mathbf{X}_i</math> from <math>\mathcal{L}</math> and add to list <math>\mathcal{L}_{OUT}</math></li> <li>(iii) <b>Case 3:</b> If <math>\mathbf{X}_i</math> is a boundary solution If (dimension of box <math>\mathbf{X}_i</math>) <math>&gt; \epsilon</math> <b>Bisect</b> <math>\mathbf{X}_i</math> into <math>\mathbf{X}_{i1}</math> and <math>\mathbf{X}_{i2}</math> Remove <math>\mathbf{X}_i</math> from <math>\mathcal{L}</math> and add <math>\mathbf{X}_{i1}</math> and <math>\mathbf{X}_{i2}</math> into the list <math>\mathcal{L}</math>. Else If (threshold dimension <math>\epsilon</math> has been reached) Remove <math>\mathbf{X}_i</math> from <math>\mathcal{L}</math> and add to list <math>\mathcal{L}_B</math> End If</li> </ul> </li> <li>(g) <b>End Case</b></li> </ul>
4	<b>End While</b>

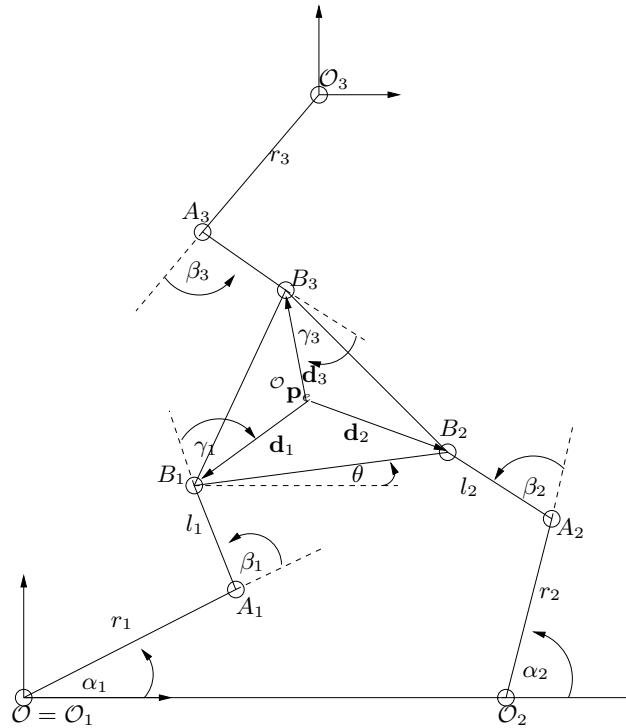


Fig. 1. A 3RRR planar parallel mechanism

a sharp solution, it can only return the sharpest box that would contain the solution. Within the box, the solution often occupies only a portion of the bounded space. The branch-and-bound strategy is therefore utilised to automate the solution search of the algorithm such that a better definition of the solution may be found. The strategy splits (bisects) the box into smaller boxes, essentially performing the evaluation of the constraints on a sub-division of the original box. Bisection is iteratively performed until an inner or outer box is found, or until a threshold dimension of the variable boxes  $\epsilon$  is reached. Boxes that remain as boundary solution at this point will form the boundary solutions of the system. In this paper, to evaluate the performance of a mechanism within the specified workspace  $\mathbf{X}$  with a specific design parameters  $\mathbf{H}$ , bisection is performed on the  $M$  dimensional interval box  $\mathbf{X}$ , where  $M$  is the number of the task space pose variables. Bisection process is performed across all the pose variables in different order, depending on the bisection algorithms. Several possible bisection algorithms are available [17].

E. Summary of Algorithm

The main skeleton of the proposed algorithm is housed in a branch-and-bound strategy summarised in Table I. List  $\mathcal{L}_{IN}$  contains the inner solutions that satisfy all the constraints in  $C(\mathbf{X}, \mathbf{H}) \leq 0$  or  $C(\mathbf{X}, \mathbf{H}) = 0$  while  $\mathcal{L}_{OUT}$  contains outer boxes, i.e. when a box fails to satisfy one or more of the constraints in  $\mathcal{C}$ . The boundary boxes are given in list  $\mathcal{L}_B$ .

IV. INTERVAL ANALYSIS ON 3RRR PLANAR PARALLEL FLEXURE MECHANISM

In this section, the workspace verification problem of a 3RRR planar flexure mechanism with respect to the given

constraints relevant to the functionality of a precision manipulator is carried out using the interval based techniques presented in Section III. The problem is to evaluate the performance of the manipulator  $C(\mathbf{X}, \mathbf{H})$ , defined by the design parameters  $\mathbf{H}$ , at the required workspace pose  $\mathbf{X}$  and to certify whether  $\mathbf{X}$  is a solution to the performance constraint. The planar workspace of the manipulator is defined as  $(x_e, y_e)^T$  for the translational motion and  $(\theta)$  for the orientation (see Fig. 1).

The performance criteria of the planar manipulator that are considered essential to the functionality of the precision manipulator are (i) the reachable workspace within the allowable deflection of the flexure joints and (ii) the workspace that yields the required motion resolution given the resolution of the joint space motion. Within the algorithm, uncertainties in the fabrication tolerance and the un-modelled kinematics of the flexure joints are taken into account in obtaining the solution. The 3RRR planar parallel mechanism, with the definitions of the variables and frame assignments, is given in Fig. 1.

In this paper, it is assumed without loss of generality that the positions of the revolute joints on the base ( $O_1, O_2, O_3$ ) and the moving platforms ( $B_1, B_2, B_3$ ) form equilateral triangles. Joint space variables are the  $(\alpha_i, \beta_i, \gamma_i)$ , where  $i = 1, 2, 3$  representing each of the three serial chains connecting the base and moving platforms. It is assumed that only joints  $\alpha_1, \alpha_2, \alpha_3$  are actuated (RRR chains) and displacement feedbacks are only available on these joints.

The manipulator in Fig. 1 was selected as an example in the following sub-sections to better illustrate the concept. The various link lengths of the selected 3RRR planar parallel

TABLE II  
PARAMETERS OF THE CASE STUDY 3RRR PLANAR PARALLEL  
FLEXURE-BASED MECHANISM.

Parameters	Values
Origin of $\mathcal{O}_1$	$(0, 0)^T$ mm
Origin of $\mathcal{O}_2$	$(167.27, 0)^T$ mm
Origin of $\mathcal{O}_3$	$(83.64, 144.86)^T$ mm
$ d_i , r_i, l_i$	10mm, 66mm, 46mm
$(x_{em}, y_{em}, \theta_{em})^T$	$(83.64, 48.29, -10.3^\circ)^T$

mechanism are summarised in Table II. The pose of the end-effector when the 3RRR mechanism is symmetrical is defined as  $(p_{em})^T = (x_{em}, y_{em}, \theta_{em})^T$ , where the subscript  $m$  denotes the ‘middle’ real value the in the interval variables. This is also assumed to be the pose when the flexure joints are at rest, i.e. when they undergo zero deflections.

#### A. Workspace by Joint Limits

It is important that the displacement of a flexure joint takes place only within the linear deformation of the joint. The selected values of the maximum allowable joint deflection used in the interval analysis of the flexure mechanism workspace should constitute a bound within which the joints behave linearly within the elastic region.

To obtain the joint displacement of the mechanism for a given end-effector pose, inverse kinematics is carried out on the desired end-effector workspace ( $\mathbf{X}$ ), with the given interval link length parameters ( $\mathbf{H}$ ). The inverse kinematics of planar parallel mechanisms was discussed in the literature [18] [19]. The inverse kinematic solution can be obtained by first calculating the angle  $\beta_i$ , which has two possible solutions within  $[0, 2\pi]$ , corresponding to elbow up or elbow down configuration of the chains. Due to the small range of joint motion in flexure mechanisms, it is only possible for it to cover one of the two solutions in its workspace. Therefore, a unique inverse kinematic solution for  $\beta_i$  can be pre-selected according to the corresponding design of the mechanism. The closed-form solution of the inverse kinematics is given as follows:

$$\cos(\beta_i) = (x_i^2 + y_i^2 - (r_i^2 + l_i^2)) / (2l_i r_i), \quad (2)$$

$$\begin{aligned} \cos(\alpha_i) &= \frac{x_i(r_i + l_i \cos(\beta_i)) + y_i l_i \sin(\beta_i)}{x_i^2 + y_i^2} \\ \sin(\alpha_i) &= \frac{-x_i l_i \sin(\beta_i) + y_i(r_i + l_i \cos(\beta_i))}{x_i^2 + y_i^2}. \end{aligned} \quad (3)$$

Obtaining the inverse cosine or inverse sine of an interval variable does not uniquely define the solution angle as these trigonometric functions are periodic. To obtain the unique solutions, both expression for  $\cos(\alpha_i)$  and  $\sin(\alpha_i)$  are utilised to specify the limit on joint  $\alpha_i$ . Bounds for the interval extension of  $\cos(\beta_i)$ ,  $\cos(\alpha_i)$  and  $\sin(\alpha_i)$  are therefore defined to reflect the deflection limits of the joints.

1) *Constraint Definition:* Interval variables  $\mathbf{p}_e = (x_e^T, y_e^T, \theta^T)^T$  were utilised to describe the desired range of the workspace. Interval variables for the link lengths, however, were used to express the fabrication tolerances and other un-modeled sources of errors. With these variables defined, the constraint for the workspace can be defined as the reachable workspace when angles  $\alpha_i, \beta_i, \gamma_i$  are all within

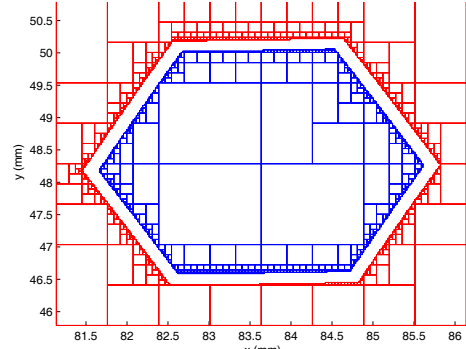


Fig. 2. Workspace of the 3RRR planar parallel mechanism, constrained by joint limits considering fabrication tolerances of  $\pm 50\mu\text{m}$  on link length  $r$  and  $l$ , taken at constant  $\theta = \theta_m = -10.3^\circ$ , with allowable flexure joint deflection of  $\pm 3^\circ$ .

the allowable joint deflections. These form the inner boxes of the workspace, while the complement form the outer boxes.

Consistency filtering is carried out by defining additional constraints derived from the set of physical constraints which form the direct kinematics of vector  $\mathbf{p}_i$ :

$$\begin{aligned} C_1(\mathbf{X}, \mathbf{H}) &= R_i \cos(\alpha_i) + L_i \cos(\alpha_i + \beta_i) - X_i = 0; \\ C_2(\mathbf{X}, \mathbf{H}) &= R_i \sin(\alpha_i) + L_i \sin(\alpha_i + \beta_i) - Y_i = 0; \\ C_3(\mathbf{X}, \mathbf{H}) &= (\cos(\alpha_i))^2 + (\sin(\alpha_i))^2 - 1 = 0; \end{aligned} \quad (4)$$

A 2B/3B consistency filtering was implemented and the results are shown in the following subsection.

#### 2) Results and Discussion: Workspace by Joint Limit:

In this example, the allowable joint deflection was set at  $\pm 3^\circ$ . The workspace to be evaluate is selected as a motion range of  $\pm 2.5$  mm in x and y direction ( $x_r = y_r = 2.5\text{mm}$ ) and  $\pm 17.5$  mrad ( $\theta_r = 1^\circ$ ) for orientation, about  $(x_{em}, y_{em}, \theta_{em})^T$ , respectively. The reachable workspace as the result of the algorithm is shown in Fig. 2. This two dimensional figure displays the inner and outer boxes of the manipulator workspace when the flexure-joint limits are imposed, after consistency filtering. It is taken at constant orientation value  $\theta = \theta_m = -10.3^\circ$ . It should be mentioned that when the same algorithm was carried out without filtering process, it failed to obtain any inner boxes of the workspace due to overestimation.

It should be noted that a fabrication error and unmodelled kinematics due to the parasitic translational motion was taken into account as being bounded within  $\pm 50\mu\text{m}$  for each link length  $r_i$  and  $l_i$ . The resulting inner boxes are therefore the guaranteed reachable workspace, with considerations to these unmodelled errors. It is therefore demonstrated that various uncertainties, including fabrication limitations, can be included in the calculation during the design process to guarantee the performance of the resulting mechanism to be within the specified requirements. It is also possible to refine this result by expressing  $L_i$  and  $R_i$  as parameters within an inner (nested) loop at the expense of higher computational time.

Figure 3 demonstrates the workspace of the mechanism bounded by the allowable joint deflection for a range of

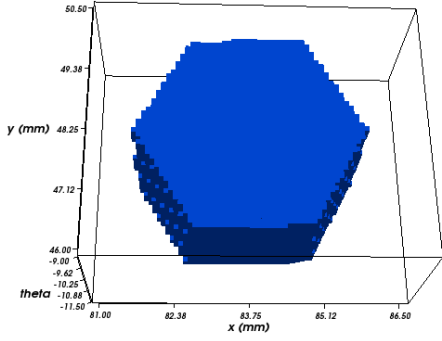


Fig. 3. The inner solution admitted into the workspace of the 3RRR planar parallel flexure mechanism, taking into account the uncertainties in the kinematic modelling and fabrication tolerances, constrained by the bounds of the allowable flexure joint deflections. The orientation range is  $\theta^Z = \theta_m \pm 17.5mrad$ .

orientation  $\Theta$ . The orientation variable is represented in the vertical-axis of the plot. The range of interval  $\Theta$  is  $\pm 17.5mrad$ .

The workspace evaluated in Fig. 2 were selected so that it was large enough to demonstrate both the inner and outer boxes of the joint deflection constraints. The available workspace can be deduced from the results by inspection. For example, from Fig. 2 and Fig. 3, it can be deduced that a translational motion of  $\pm 1mm$  in  $x$  and  $y$  direction can be achieved throughout an orientation range of  $\pm 17.5mrad$ , even with a fabrication tolerance of  $\pm 50\mu m$ .

### B. Task Space Motion Resolution

As flexure mechanisms are generally employed for precision manipulation, the resolution of the smallest step possible in the motion of the end-effector is often an important performance criterion. Generally, it is possible to directly establish the bounds of joint space motion resolutions from the specifications of the sensors and actuators used. Incremental step size in task space can therefore be calculated by the differential kinematic relationship with the incremental step size in joint space displacement.

$$\mathbf{J}_1 \cdot \Delta \mathbf{x}_e = \mathbf{J}_2 \cdot \Delta \mathbf{q}, \quad (5)$$

where  $\Delta \mathbf{q}$  is the incremental joint space displacement (or in this case, resolution). In this example of 3RRR, we consider the incremental motion of the base joints  $\Delta \mathbf{q} = (\Delta \alpha_1, \Delta \alpha_2, \Delta \alpha_3)^T$ . It is then required to solve for  $\Delta \mathbf{x}_e$  in the linear equation (5).

The differential kinematic relationships can be obtained from [18] as

$$\begin{bmatrix} \mathbf{f}_i^T & \mathbf{f}_i^T \mathbf{d}_i^\perp \end{bmatrix} \begin{bmatrix} \dot{\mathbf{p}}_e \\ \omega \end{bmatrix} = r_i \mathbf{f}_i^T \begin{bmatrix} -\sin(\alpha_i) \\ \cos(\alpha_i) \end{bmatrix} \dot{\alpha}_i, \quad (6)$$

where  $\mathbf{f}_i^T$  is the unit vector in the direction of the reciprocal screws passing through the revolute joints at points A and B:

$$\mathbf{f}_i^T = \frac{1}{l_i} \begin{bmatrix} x_i - r_i \cos(\alpha_i) \\ y_i - r_i \sin(\alpha_i) \end{bmatrix} \quad (7)$$

and  $\mathbf{d}_i^\perp$  is the vector perpendicular to  $\mathbf{d}_i$ , or  $\mathbf{d}_i^\perp = (-d_{iy}, d_{ix})^T$ . The overall differential kinematics of the

mechanism can be described by:

$$\mathbf{J}_1 \cdot \dot{\mathbf{x}}_e = \mathbf{J}_2 \cdot \dot{\boldsymbol{\alpha}} \quad (8)$$

where  $\dot{\mathbf{x}}_e = (\dot{\mathbf{p}}_e^T, \dot{\omega})^T = (\dot{x}_e, \dot{y}_e, \dot{\theta})^T$  and  $\mathbf{J}_1, \mathbf{J}_2$  are the  $3 \times 3$  Jacobian matrices, with each row representing the relationship (6) for individual leg  $i$ . Note that  $\mathbf{J}_2$  is a diagonal matrix.

1) *Constraint Definition*: The constraint to be satisfied is therefore defined as:

$$\{\forall \mathbf{x} \in \mathbf{X}, \forall \mathbf{h} \in \mathbf{H}, |\Delta \mathbf{X}_e| \leq \Delta \mathbf{X}_{threshold}\}, \quad (9)$$

where  $\Delta \mathbf{X}_e$  is the interval extension of vector  $\mathbf{x}_e$  as defined in (5). Inner solution is obtained when the specified workspace satisfies (9) while outer box is obtained when  $\Delta \mathbf{X}_e \notin \Delta \mathbf{X}_{threshold}$ .

For this example, it is given that joint space displacement resolution is bounded within 0.06 mrad. The desired resolution ( $\Delta \mathbf{X}_{threshold}$ ) for the task space translational motion and orientation are set at  $0.5\mu m$  and  $0.5mrad$ , respectively.

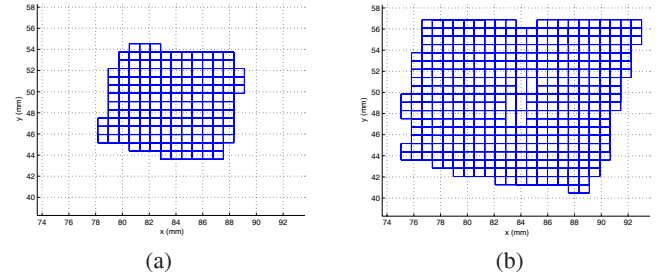


Fig. 4. Two dimensional workspace at constant  $\theta = \theta_m = -10.3^\circ$  that satisfies the required motion requirement, given the joint space motion resolution. Solving algorithms were (a) preconditioned Hansen-Bliek and (b) symbolic preconditioning with Gaussian elimination.

2) *Results and Discussion: Task Space Resolution*: When (5)-(9) is evaluated for the workspace of our 3RRR planar parallel manipulator, the workspace that satisfies the required motion resolution is given in Fig. 4(a). The solution was obtained through the Hansen-Bliek solving algorithm [20], [21], which is numerically pre-conditioned.

Further improvement can be obtained through symbolic preconditioning, as proposed in [22]. This approach is possible when symbolic expressions of the linear system of equations is given. The idea is to minimise symbolically the number of multiple occurrences of each variable. This method is performed by evaluating matrix  $\mathbf{M}$  but keeping  $\mathbf{J}_1$  symbolic. This allows the elements of the resulting matrix to be rearranged symbolically to minimise the multiple occurrences of various interval variables, hence reducing the effect of dependency. Consistency filtering is also included in the algorithm to further sharpen the results. The improvement in the algorithm ability to admit inner solution is demonstrated in the amount of workspace that can be certified as the inner solution of the constraint dictated by the desired end-effector motion resolutions (Fig. 4(b)). The results in Fig. 4 were obtained with the exact same conditions, taken at constant  $\theta = \theta_m$ , with the only difference being the algorithm for solving the linear equations: (a) the preconditioned Hansen-Bliek algorithm, and (b) the symbolically preconditioned Gaussian elimination method.

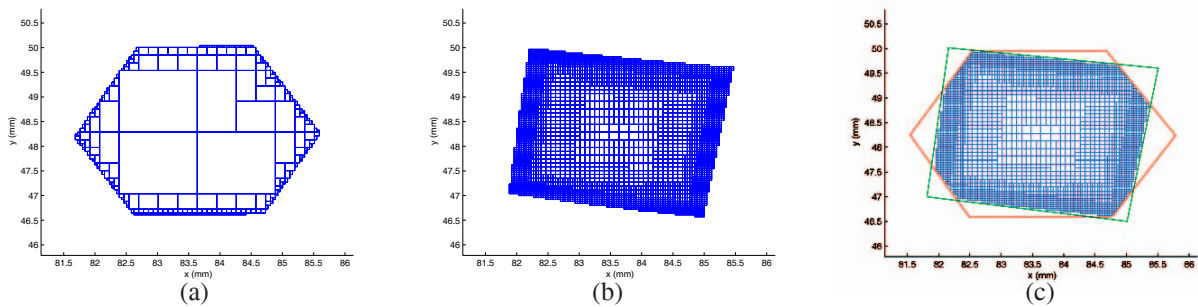


Fig. 5. (a) The workspace allowable by limits of joint deflection. (b) The workspace that satisfies the required motion resolution. (c) The intersection of all given constraints.

### C. Overall Available Workspace

The certified available workspace of the planar parallel mechanism can be evaluated by imposing both the joint displacement constraint and the motion resolution constraint. For the desired workspace to satisfy all the performance required of the manipulator, it is necessary that the procedure results in inner solutions to all the given constraints. To be an outer box, however, it needs only to be an outer box to any of the constraint.

An example of the usable workspace that satisfies both the criteria (joint limit and required motion resolution) is therefore given by Fig. 5. The workspace allowed by the joint limit is shown in Fig. 5 (a), the workspace that produces required end-effector motion resolution of  $0.5\mu\text{m}$  (translation) and  $0.5\text{mrad}$  (orientation), given joint motion resolution ( $\Delta\alpha_i$ ) of  $0.05\text{mrad}$ , is given in Fig. 5(b) and the resulting intersection, which is the workspace that satisfies all the given criteria, is given in Fig. 5(c).

Setting the orientation  $\theta$  as an interval would evaluate the constraints for a range of value of orientation. The resulting workspace is guaranteed to satisfy all the given criteria. To test a desired workspace  $\mathbf{X}$ , with a particular manipulator design and link lengths  $\mathbf{H}$ , the interval variables of the workspace can be substituted directly into the algorithm and certified whether it is an inner solution of the constraints. If bisection is required in certifying this, then it is necessary that all the resulting (smaller) interval boxes constituting  $\mathbf{X}$  are certified as inner solutions.

## V. CONCLUSIONS

A technique to address workspace verification problem of a precision flexure-based mechanism is presented in this paper. The technique certifies whether or not the required workspace satisfies certain performance criteria, taking into account modelling and fabrication uncertainties. Performance features relevant to a flexure-based mechanism were presented and the efficient interval-based methods in evaluating and resolving the features were proposed, implemented, and discussed. Future work is aimed at extending the algorithm to produce an efficient synthesis algorithm that would enable the determination of design parameter intervals of a mechanism that satisfy a set of given constraints.

## REFERENCES

- [1] J. M. Paros and L. Weisbord, "How to design flexure hinge," *Machine Design*, vol. 37, no. 27, pp. 151–156, 25 November 1965.
- [2] F. E. Scire and E. C. Teague, "Piezodriven  $50\text{-}\mu\text{m}$  range stage with subnanometer resolution," *Rev. Sci. Instr.*, vol. 48, no. 12, pp. 1735–1740, December 1978.
- [3] D. Choi and C. Riviere, "Flexure-based Manipulator for Active Handheld Microsurgical Instrument," *Procs. IEEE Conf. Engineering in Medicine and Biology Society*, pp. 2325–2328, Sept. 2005.
- [4] D. Kim, D. Kang, J. Shim, I. Song, and D. Gweon, "Optimal design of a flexure hinge-based XYZ atomic force microscopy scanner for minimizing Abbe errors," *Rev. Sci. Instr.*, July 2005.
- [5] B.-J. Yi, G. B. Chung, H. Y. Na, W. K. Kim, and I. H. Suh, "Design and experiment of a 3-dof parallel micromechanism utilizing flexure hinges," *IEEE Trans. Robs. & Autom.*, vol. 19, no. 4, pp. 604–612, August 2003.
- [6] J.-P. Merlet, C. Gosselin, and N. Mouly, "Workspaces of planar parallel manipulators," *Mech. Mach. Theory*, vol. 33, no. 1/2, pp. 7–20, 1998.
- [7] G. Pennock and D. Kassner, "The workspace of a general geometry planar three degree of freedom platform manipulator," *ASME J. Mechanical Design*, vol. 115, no. 2, pp. 269–276, 1993.
- [8] V. Kumar, "Characterization of workspaces of parallel manipulators," *ASME J. Mechanical Design*, vol. 114, no. 3, pp. 368–375, 1992.
- [9] N. Lobontiu, *Compliant Mechanisms: Design of Flexure Hinges*. CRC Press, 2002.
- [10] T.-F. Niaritsiry, N. Fazenda, and R. Clavel, "Study of the sources of inaccuracy of a 3 DOF flexure hinge-based parallel manipulator," in *Procs. IEEE Intl. Conf. Robs. & Autom.*, vol. 4, 2004, pp. 4091–4096.
- [11] R. Moore, *Interval Analysis*. Prentice-Hall, NJ., 1966.
- [12] E. Hansen and G. Walster, *Global Optimization using Interval Analysis*, 2nd ed. Marcel Dekker, NY., 2004.
- [13] F. Benhamou, F. Goualard, and L. Granvilliers, "Revising hull and box consistency," in *Procs. Intl. Conf. on Logic Programming*, Las Cruces, USA, 1999, pp. 230–244.
- [14] M. Collavizza, F. Delobe, and M. Rueher, "Comparing partial consistencies," *Reliable Computing*, vol. 5, pp. 1–16, 1999.
- [15] O. Lhomme, "Consistency techniques for numeric CSPs," in *Procs. IJCAI 93*, Chambéry, France, August 1993, pp. 232–238.
- [16] A. Neumaier, *Interval Methods for Systems of Equations*. Cambridge University Press, London, 1990.
- [17] R. B. Kearfott, "Corrigenda: Some tests of generalized bisection," *ACM Transactions on Mathematical Software*, vol. 14, no. 4, p. 399, 1988.
- [18] I. Bonev, "Geometric analysis of parallel mechanisms," Ph.D. dissertation, Université Laval, Québec, QC, Canada, 2002.
- [19] J.-P. Merlet, *Parallel Robots*. Dordrecht: Kluwer, 2000.
- [20] J. Rohn, "Cheap and tight bounds: The recent result by E. Hansen can be made more efficient," *Interval Computations*, vol. 4, pp. 13–21, 1993.
- [21] A. Neumaier, "A simple derivation of the Hansen-Bliok-Rohn-Ning-Kearfott enclosure for linear interval equations," *Reliable Computing*, vol. 5, no. 2, pp. 131–136, 1999.
- [22] J.-P. Merlet and P. Donelan, "On the regularity of the inverse jacobian of parallel robot," in *Proceedings of the International Symposium of Advances in Robot Kinematics (ARK)*, Ljubljana, Jun 2006, pp. 41–48.